Original Research Article

Evaluation of the influence on the use of additional filtration in pelvic radiographic examinations using a phantom object

ABSTRACT

Aims: This study aimed to determine the effect of additional filtration on the image quality and dose reduction in pelvic radiographic examinations.
Study design: Mention the design of the study here.
Place and Duration of Study: The research was conducted at a municipal emergency service radiology department in Rio Grande do Sul, Brazil.
Methodology: Using a simulator object to replicate clinical examination conditions. The radiographic equipment was fitted with aluminum, copper, and copper-aluminum composition filters to identify the optimal filtration for reducing radiation doses and maintaining image quality.
Results: Results showed that filtration effectively reduced dose and average absorbed dose in internal organs, with the greatest reduction observed with the copper filter. However, excessive filtration resulted in a decrease in image quality, particularly with the copper filter. The Figure of Merit (FOM) demonstrated that keeping the electrical factors of the X-ray tube consistent (70 kVp and 32 mAs) and using an additional 2.5 mmAl filter could optimize pelvic radiographic examinations, based on the diagnostic IQ criteria established by the service.
Conclusion: In conclusion, the FOM revealed that using additional filtration of 2.5 mmAl and maintaining the X-ray tube's electrical factors at 70 kVp and 32 mAs could reduce the KERMA in air by 49.8% in the patient, 41.5% in the testes, 35.5% in the bladder, 30.4% in the ovaries, 29.7% in the bone marrow, and 35.3% in the total effective dose of the examination, while maintaining equivalent image quality.

Keywords: [X-rays, Filtration, Digital Radiography, Patient Safety, Radiation Dose}

1. INTRODUCTION

Pelvic radiography is one of the most frequently requested exams by physicians for patients who are victims of trauma or traffic accidents. This region houses much of the bone marrow (40%) and the gonads (100%), which are highly radiosensitive [1].
Recently, Alzyoud et al. [2], and Hamid [3], reported in their studies that the pelvis radiographic examination represents the second highest radiation dose contributor to the patient.
Traditionally, the use of additional filtration is associated with decreased radiographic contrast and image quality (IQ). Although, in SD there is no fixed relationship between the radiation dose and the resulting optical density in the image as in the screen-film system, so radiographic contrast is optimized by image post-processing features [4-6]. The parameter

used as a variable in this study is the relationship between radiation dose and IQ, i.e., increasing beam filtration results in dose reduction and change in standard IQ.
The quality of the images was evaluated using public domain software, ImageJ [7], to determine between the regions of interest (ROI) the signal and noise. With the results obtained, the signal noise ratio (SNR) and contrast noise ratio (CNR) were calculated. These IQ descriptors have been successfully used as an IQ measure in several optimization studies [4,8,9].
This study aims to evaluate the influence of additional filtration on IQ and dose reduction in pelvis radiographic examinations. Finally, a relationship between radiation dose and IQ will be presented.

2. MATERIAL AND METHODS / EXPERIMENTAL DETAILS / METHODOLOGY

2.1 Equipment

In this study a LOTUS radiographic equipment, model HF630, operated with a high frequency generator [10] was used. The coarse focal point (1.2 mm^2) was chosen because it is suitable for pelvis examinations. The images were obtained with a 10:1 grid ratio (52 lines/cm) and the image receptor source distance (SRD) of 1 meter in the cassette drawer. To capture the digital images, an Agfa computed radiology (CR) system was used, consisting of a 35 cm x 43 cm cassette, image plate (IP) with a spatial resolution of 10 pixels / mm and a resolution scale of 16 bits / pixel. The images were viewed on the monitor of the system's own workstation [11]. Measurements of the radiation beam, K_{AIR}, were performed with a UNFORS Xi R/F solid-state detector [12] calibrated in a reference laboratory.

2.2 Simulator Object

We used a phantom object (OS) consisting of a plastic box measuring 39 x 26 x 22 cm^3 (length, width and height, respectively), used for quality control in bone densitometry equipment. The box was filled with water to a height of 15 cm, without a lid, with direct access through the water surface. To assess IQ and simulate anatomical tissues, structures were included to produce contrast in the radiographic image. The structures were a 10-step aluminum (Al) ladder with thicknesses of 5.5; 8.7; 11.7; 14.7; 17.7; 20.6; 23.9; 26.6; 29.6 and 32.6 mm; and a 0.8 mm-thick Al plate with 8 holes in 2 sets of 6.0 mm, 4.5 mm, 3.0 mm and 1.5 mm diameter, MRA brand, model CQ-07, N/S 08-145. Figure 1 shows the two devices:

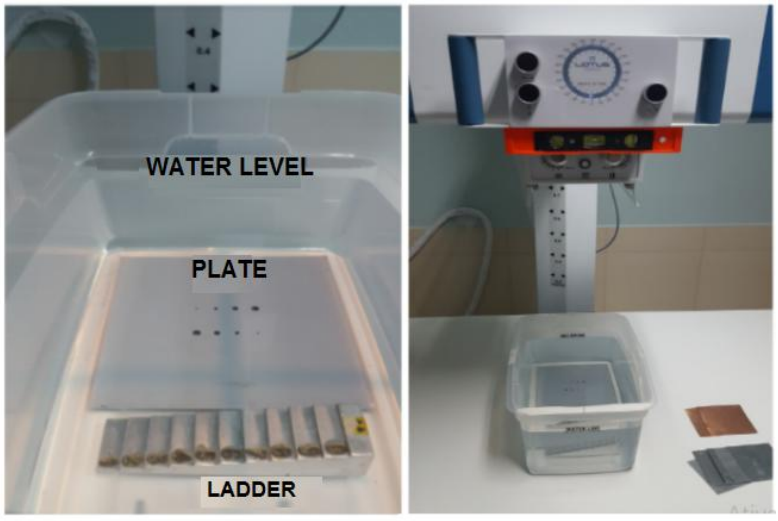

(a) (b)

Fig. 1 - Structures submerged in water and the positioning of the OS for image acquisition.

Source: from Author (2023). Figure (1a) identifies the centralized OS with the central beam for the X-ray beam. Figure (1b) shows acquisition of the reference image without additional filtration, in detail the filters used in the research, five Al and two copper foils.

2.3 Filters

To verify the influence of filtration, a set of 7 filters were used, arranged in the following combination (Table 1). Five 10 x 10 cm^2 aluminum plates 0.5 mm thick and two 10 x 10 cm^2 copper plates 0.29 mm thick inserted in the collimation box of the radiographic equipment were used. The Filtration Index (FI) was defined for each set of plates. The denomination FI1 represents the original beam, without filtration, with only the total head filtration of 2.75 mmAl as obtained during the quality control tests.

Table 1 - Identification of the FI, quantity of plates and final thickness of the added material

FI	Plates	Final thickness
1	-	No Additional Filtration
2	1 x Al	+0.5 mmAl
3	2 x Al	+1.0 mmAl
4	3 x Al	+1.5 mmAl
5	4 x Al	+2.0 mmAl
6	5 x Al	+2.5 mmAl
7	1 x Cu	+0.29 mmCu
8	1 x Cu + 1 x Al	+0.29 mmCu + 0.5 mmAl
9	1 x Cu + 2 x Al	+0.29 mmCu + 1.0 mmAl
10	1 x Cu + 3 x Al	+0.29 mmCu + 1.5 mmAl
11	1 x Cu + 4 x Al	+0.29 mmCu + 2.0 mmAl
12	1 x Cu + 5 x Al	+0.29 mmCu + 2.5 mmAl
13	2 x Cu	+0.58 mmCu

Source: from the Author (2023).

Initially, all quality control (QC) tests of the radiographic equipment and the CR system were performed according to the current legislation [13]. The radiographic equipment was used to obtain the OS images and measure the radiation dose and the CR system was used for image detection.

2.4 Image acquisition and radiation dose measurement experimental

During the acquisition of the images of the phantom object (OS) and measurement of the radiation dose (Figure 2), the exposure factors were kept constant with the standard technique used in the service for pelvis examinations, and plates of varying thicknesses of Al and Cu were exchanged. According to the setup shown in Figure (2a), the OS was exposed twice and 2 images were obtained for each filtration (FI). A total of 26 images of the OS were generated, and these were identified in the lower left quadrant of the images. All images were acquired using the same 35 cm x 43 cm cassette placed in the table Bucky, avoiding

variations in the acquisition of the latent image, using the CR system processed by the cassette reader, model CR 30-X.

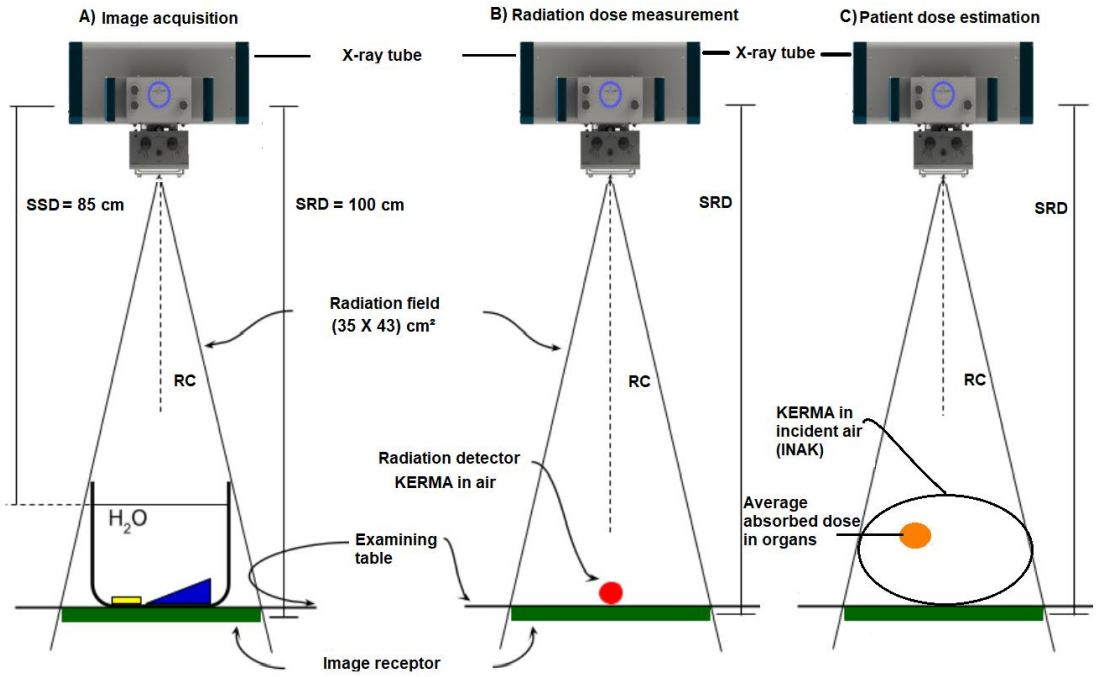

Fig. 2 - Exposure geometry for OS imaging and radiation dose measurement.

Figure (2a) illustrates the irradiation geometry with a simulator object for imaging, where SSD is the source distance water surface, SRD is the source-image-receptor distance, and RC is the central radius of the collimator light field. The objects are Al plates (yellow) and step ladder (blue). Figure (2b) illustrates the irradiation geometry for obtaining dose. The detector is in red. Figure (2c) shows two magnitudes for estimating the dose to the patient. Source: The author's own (2023)

For the evaluation of KERMA, a total of 52 exposures were performed in groups of four measurements of K_{AIR} for each FI, and the mean value and the standard deviation (SD) of the group were calculated to reduce the random error. From the calculated value of K_{AIR} was possible to obtain the value of the Incident Air Kerma (INAK) at 1m. For any distance, the INAK can be obtained by correcting the obtained value by the inverse of the square of the distance, as shown in equation 1.

$$INAK = K\_AIR \times (SRD/SSD)^2 \quad (1)$$

where SRD is the image receiver focus distance (100 cm), and SSD is the surface focus distance (85 cm), as illustrated in Figure 2(b).

2.5 Absorbed Dose and Effective Dose (E)

We used the software PCXMC 2.0 [14], which is a program that uses the Monte Carlo method, which is a statistical method that relies on massive random sampling to obtain numerical results, to calculate the radiation dose to internal organs and the effective dose of the patient adjusted to the radiographic exam. From the insertion of voltage data (70 kV), anode angle (12.5°), and total HVL of the equipment (2.75 mmAl) the dose to the main

internal organs of the pelvis region and the effective dose for each FI was estimated. The plates used as filters are inserted as additional filtration to the PCXMC, as well as the respective calculated INAK for adjustment in the dose calculated by the program.

2.6 Image Quality

Figure (3a) identifies the location of each ROI, with ROIs #1 through #10 representing the rungs of the aluminum ladder, ROI#11 representing the image background, ROI#12 referring to the plate. In Figure (3b) in the image detail of the plate, ROI#13 parallel to the hole and ROI#14 encompassing part of the 6.0 mm hole of the smooth plate. All rectangular ROIs are of the same area (1 254 mm²), with the exception of ROI#14 (125 mm²) that encompasses part of the 6 mm hole of the plate.

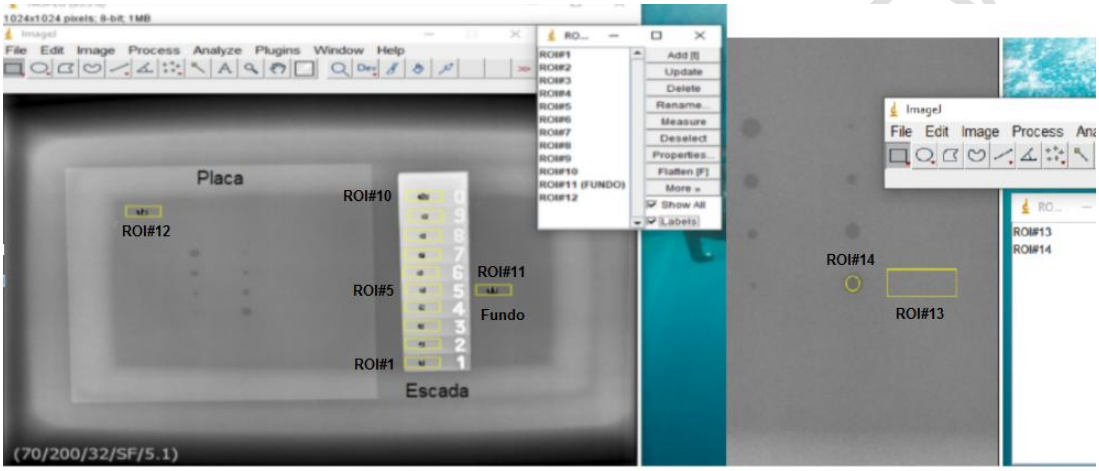

Fig. 3 - Location of the ROIs in the reference image, without filtration (FI1), in the *ImageJ* program
Source: from the Author (2023).

2.7 Signal and Noise Evaluation

The quality of the images was evaluated using public domain software, *ImageJ* (WAYNE, 2021). To determine between the regions of interest (ROI) the signal and noise of the two images obtained for each FI. To evaluate the stair contrast, it was defined as the signal difference between adjacent stair steps taken two by two, i.e. the signal value from ROI#2 - ROI#1, ROI#3 - ROI#2, to ROI#10 - ROI#9 for each FI, according to [15]. For evaluation of the plaque contrast, the difference between the signal value of ROI#13 and ROI#14 was chosen.
With the results obtained, the signal-to-noise ratio (SNR) and contrast-to-noise ratio (CNR) were calculated. In order to have a better IQ analysis, the SNR and CNR of ROI#5 and ROI#12 were calculated. These ROIs were chosen by the difference in thickness between them, for ROI#5 (17.7 mm) and ROI#12 (0.8 mm) which simulates the different thickness of the bones in the pelvis region, according to equation 2 and equation 3, respectively.

$$SNR = (pixel\ average)/(standard\ deviation) \quad (2)$$

$$CNR =$$

$$|(Average\ of\ the\ signal\ values\ (Background)\ -\ Average\ of\ the\ signal\ values\ (ROI))/(Standard\ Deviation\ (Background))| \quad (3)$$

2.8 Optimization: Figure of Merit (FOM)

FOM quantifies the relationship between IQ, here taken as CNR, and effective dose, and is applied in order to help verify the influence of the filter when considering the two parameters simultaneously, as per equation 4:

$$FOM = CNR/(effective\ dose\ (E)\ ) \quad (4)$$

2.9 Selection Criteria

Since there are no reference values to define the limits of IQ descriptors, we considered as "reference" values those measured in the reference images, acquired with the standard technique used in the service and without filtration (FI1). We chose the percentage deviation (D%) to compare the acquired images in relation to the reference image, according to equation 5:

$$D(\%) = ((new\ value)/(Standard\ Value)) - 1 \quad (5)$$

3. RESULTS AND DISCUSSION

The results of constancy of the radiographic equipment showed that the error, less than 6% in the worst case, is below the 10% accepted as a limit in the legislation, which guarantees it good reproducibility. The minimum limit for half value layer (HVL) at 80 kVp is 2.9 mmAl, and as it was found 3.13 mmAl, the equipment complies with the legislation (BRASIL, 2019).

3.1 Beam Quality (HVL) and KERMA in Air

Initially, with the selected standard technique, HVL and K_{AIR} values were measured, as illustrated in Figure (2b), for each FI. Table 2 lists the mean values of the HVL (mmAl) and K_{AIR} (mGy) readings, as well as the values for the percentage deviation (D%) of HVL and K_{AIR} relative to FI1.

Table 2 - CSR values (mmAl) and radiation dose (mGy) as a function of FI

	Added filtration	HVL*		K_{AIR*}	
FI	**Thickness and material**	**mmAl**	**D%**	**mGy**	**D%**
1	No Additional Filtration	2,75	-	1,64	-
2	+0.5 mmAl	2,89	5,1%	1,40	-14,7%
3	+1.0 mmAl	3,01	9,5%	1,23	-24,8%
4	+1.5 mmAl	3,14	14,2%	1,08	-34,0%
5	+2.0 mmAl	3,35	21,8%	0,96	-41,6%
6	+2.5 mmAl	3,61	31,3%	0,82	-49,8%
7	+0.29 mmCu	4,72	71,6%	0,34	-79,3%
8	+0.29 mmCu + 0.5 mmAl	4,81	74,9%	0,29	-82,3%
9	+0.29 mmCu + 1.0 mmAl	4,92	78,9%	0,27	-83,4%
10	+0.29 mmCu + 1.5 mmAl	4,96	80,4%	0,26	-84,4%

11	+0.29 mmCu + 2.0 mmAl	5,16	87,6%	0,25	-85,0%
12	+0.29 mmCu + 2.5 mmAl	5,32	93,5%	0,22	-86,4%
13	+0.58 mmCu	6,15	123,6%	0,13	-92,1%

Source: from Author (2023). *The largest standard deviation, of the 4 measures, was 2.2% for FI7 and the others were below 1%.

The measured results corroborate what was expected, that with increased filtration the beam quality (HVL) rises, making the beam more penetrating and reducing the radiation dose (K_{AIR}). As expected, as Al plates were added, a slow reduction in K_{AIR} value was observed as a function of the additional thickness, up to a maximum of 2.5 mmAl corresponding to FI6 (49.8%). However for FI7, with the introduction of copper (0.29 mmCu), an abrupt reduction of K_{AIR} (79.3%) is noted due to the change of material. This behavior is due to the differences in density and energy absorption coefficient between the materials. This situation is expected, because copper is 3x denser than aluminum, besides having an atomic mass 2x greater, which provides a much higher probability of interaction with the photons. For FI indices 8, 9, 10, 11 and 12, the reductions were 82.3%, 83.4%, 84.4%, 85.0% and 86.4%, respectively. A second significant K_{AIR} reduction is obtained for FI13 (92.1%) corresponding to the insertion of a new Cu plate (+0.58 mmCu) in place of the Al plates.
It turns out that one copper foil is more efficient than several aluminum foils, and that placing aluminum foils together with the copper foil causes a small effect, especially after the insertion of the Cu plate (at most 2% reduction for 0.5 mm Al).
In Figure 4, the 13 X-rays for each OS IF are shown. It can be seen that, visually, the influence of filtration for this type of OS on IQ is very small. Overall, one notices little difference between the steps of the ladder and between the holes in the plate from images obtained with a dose of 1.64 mGy (no filtration) to a minimum dose of 0.13 mGy (maximum filtration). This analysis shows that improving diagnostic accuracy through overexposure may not be the best strategy, as improved visualization of anatomical structures of interest may not be achieved with more doses alone.

FI1 reference image (without additional filtration)

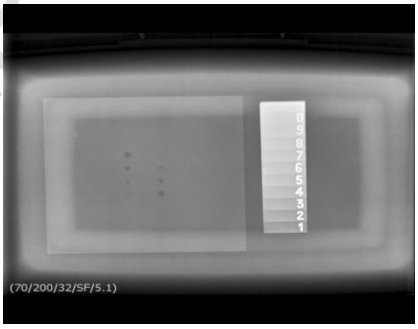

FI2 (+0.5 mmAl) FI3 (+1.0 mmAl) FI4 (+1.5 mmAl)

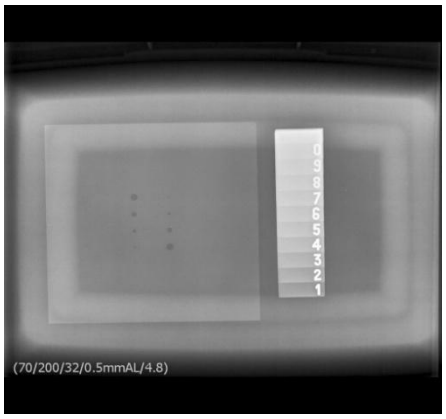

FI5 (+2.0 mmAl)

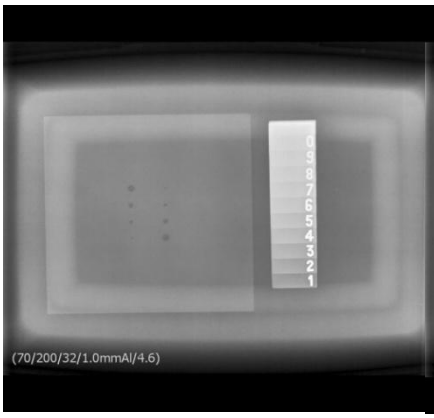

FI6 (+2.5 mmAl)

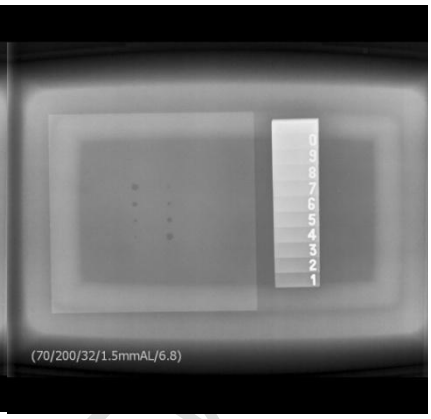

FI7 (+0.29 mmCu)

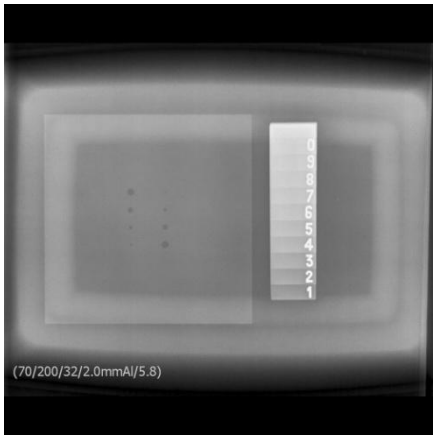

FI8 (+0.29 mmCu + 0.5 mmAl)

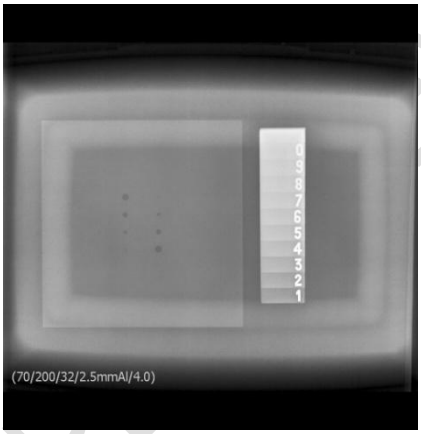

FI9 (+0.29 mmCu + 1.0 mmAl)

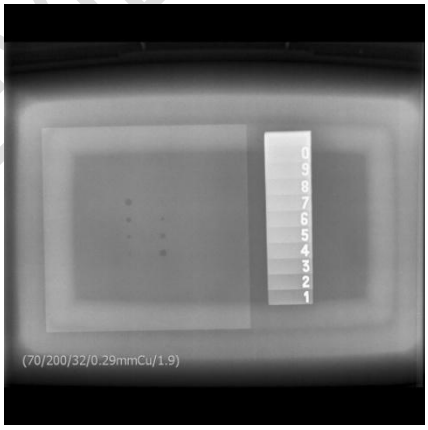

FI10 (+0.29 mmCu + 1.5 mmAl)

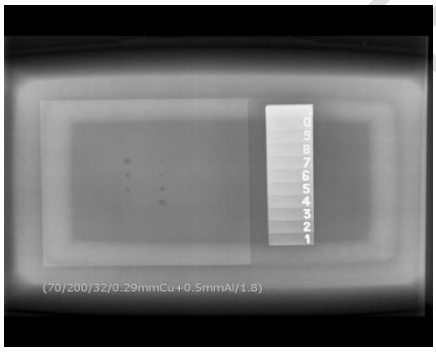

FI11 (+0.29 mmCu + 2.0 mmAl)

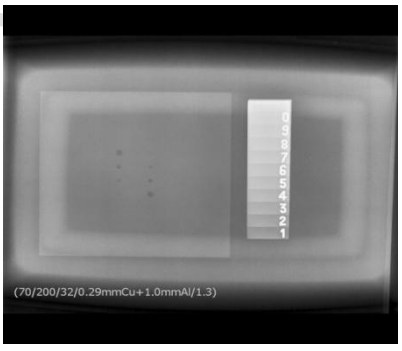

FI12 (+0.29 mmCu + 2.5 mmAl)

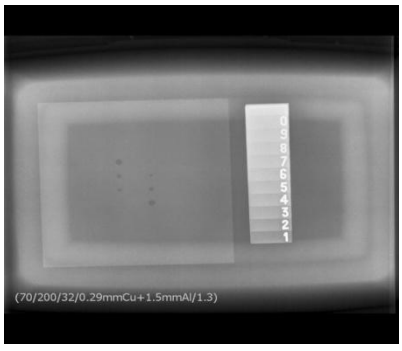

FI13 (+0.58 mmCu)

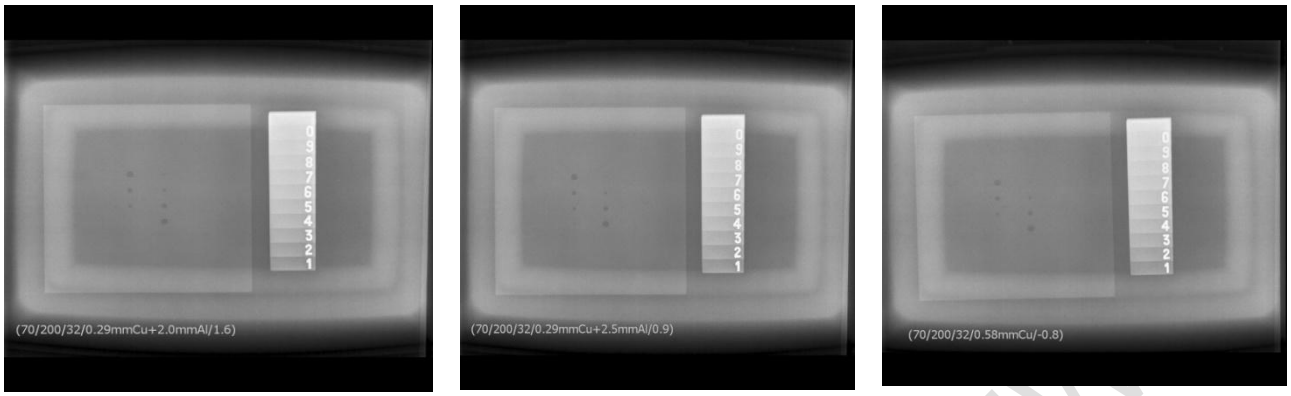

Fig. 4 - Reference image and acquired images for each FI

Source: from the Author (2023). The values at the foot of each image are respectively the kVp, mA, mA.s, additional filtration type, and exposure index.

3.2 Image Quality (IQ)

Tables 3 and 4 show the mean values of signal and noise, respectively, referring to the 10 steps of the ladder (ROI#1 to ROI#10), the background (ROI#11) and the plate (ROI#12, ROI#13 and ROI#14) as a function of the FI. In Table 5, one can compare the results concerning the percentage deviation (D%) from the reference image for the IQ descriptors (signal, noise, SNR, CNR) for ROI#5 of the stairs and ROI#12 of the plate.

Table 3 - Signal value for each ROI of the ladder, plate and bottom

	Stair Step										Fund	Plate		
FI	1	2	3	4	5	6	7	8	9	10	11	12	13	14
1	165,4	177,7	186,2	195,1	201,3	204,9	207,9	209,9	212,2	216,6	112,2	134,9	131,9	111,2
2	160,8	171,8	182,4	191,3	197,5	203,3	206,5	208,4	211,0	215,3	111,8	135,6	130,2	110,5
3	160,5	171,2	180,9	190,3	195,3	201,0	204,1	206,2	209,1	213,7	112,5	135,6	132,1	113,0
4	162,6	172,1	180,9	190,3	196,2	200,7	204,0	206,3	209,3	212,2	113,0	135,6	131,4	113,2
5	162,9	172,7	181,5	190,0	196,1	200,6	204,6	205,7	208,3	211,9	114,2	135,3	129,5	111,7
6	164,6	176,3	184,8	192,6	198,5	202,4	205,8	207,0	209,2	213,2	114,2	134,1	130,8	110,7
7	162,7	175,3	183,7	192,0	198,5	202,8	206,3	207,7	210,2	213,4	113,9	134,1	127,4	109,6
8	160,4	171,6	180,4	190,5	196,1	200,8	205,7	207,7	210,7	213,9	114,0	136,1	129,6	113,3
9	154,6	164,4	174,8	184,9	192,3	198,8	203,2	206,3	209,9	212,9	112,2	138,0	128,7	112,7
10	156,4	168,9	179,4	188,5	194,2	199,2	203,1	204,6	207,5	212,1	112,5	135,2	129,4	112,8
11	153,2	163,3	175,2	185,4	192,8	199,7	204,2	207,4	210,9	215,5	112,1	137,8	129,1	113,1
12	155,1	165,5	176,3	187,2	192,2	198,5	203,0	205,2	208,7	212,7	112,8	132,2	129,1	113,2
13	155,9	169,5	179,9	189,9	196,2	201,1	205,4	207,5	210,3	214,9	114,3	136,5	127,7	113,2

Source: from the Author (2023).

Table 4 - Noise value for each ROI of the ladder, plate and background

	Ladder										Fund	Plate		
FI	1	2	3	4	5	6	7	8	9	10	11	12	13	14
1	4,9	4,5	3,9	3,7	3,6	3,3	3	2,9	2,9	2,9	2,1	2,6	2,4	1,9

2	5,3	4,8	4,1	3,8	3,5	3,3	3,1	2,8	2,8	2,9	2,4	2,5	2,2	2,2
3	5,7	4,7	4,0	3,9	3,7	3,3	3,1	2,7	2,8	3,0	2,5	2,2	2,2	2,1
4	5,4	4,7	4,0	3,5	3,5	3,3	2,9	2,9	2,7	2,9	2,3	2,3	2,2	2,2
5	5,2	4,5	4,0	3,7	3,6	3,3	3,1	3,1	2,9	2,8	2,5	2,6	2,2	2,1
6	5,1	4,6	4,0	3,5	3,6	3,5	3,2	3,0	2,8	3,0	2,2	2,5	2,3	2,0
7	5,5	4,9	4,5	4	4,2	3,9	4,1	3,6	3,4	3,4	2,4	2,8	2,6	2,6
8	5,3	5,1	4,6	4,5	4,3	4,2	4,1	3,6	3,5	3,3	2,5	2,7	2,6	2,4
9	6,1	5,3	4,7	4,6	4,3	4,2	4,5	3,8	3,7	3,6	2,8	2,7	2,6	2,3
10	5,0	5,3	4,6	4,5	4,3	4,3	3,8	3,6	3,5	3,5	2,7	2,8	2,6	2,7
11	5,5	5,1	4,7	4,7	4,2	4,2	3,8	3,6	3,4	3,6	2,9	2,8	2,6	2,3
12	5,1	5,2	4,6	4,8	4,7	4,4	4,0	3,8	3,7	3,6	2,9	2,7	2,6	2,3
13	4,9	5,4	5,0	4,8	4,8	4,5	4,3	4,0	4,0	3,9	3,0	3,4	2,8	2,7

Source: from the Author (2021)

Table 5 - Percent deviation, relative to the reference image, of dose and IQ for each FI

		Ladder (ROI#5)				Plate (ROI#12)			
FI	**added filtration**	**signal**	**noise**	**SNR**	**CNR**	**signal**	**noise**	**SNR**	**CNR**
2	+0.5 mmAl	-1,9%	-1,3%	0,9%	-15,7%	0,5%	-3,8%	4,4%	-8,1%
3	+1.0 mmAl	-3,0%	2,8%	-5,6%	-21,3%	0,5%	-15,4%	18,7%	-13,9%
4	+1.5 mmAl	-2,6%	-2,5%	0,3%	-15,6%	0,5%	-11,5%	13,7%	-10,5%
5	+2.0 mmAl	-2,6%	1,4%	-2,6%	-22,6%	0,3%	0,0%	0,2%	-21,8%
6	+2.5 mmAl	-1,4%	-0,2%	-1,4%	-10,8%	-0,6%	-3,8%	3,3%	-17,3%
7	+0.29 mmCu	-1,4%	18,1%	-15,5%	-17,8%	-0,6%	7,7%	-7,7%	-23,1%
8	+0.29 mmCu + 0.5 mmAl	-2,6%	20,1%	-18,4%	-21,0%	0,9%	3,8%	-2,9%	-16,4%
9	+0.29 mmCu + 1.0 mmAl	-4,5%	20,2%	-20,0%	-33,2%	2,3%	3,8%	-1,5%	-15,7%
10	+0.29 mmCu + 1.5 mmAl	-3,5%	19,4%	-19,2%	-27,5%	0,2%	7,7%	-6,9%	-21,2%
11	+0.29 mmCu + 2.0 mmAl	-4,3%	17,7%	-17,9%	-33,6%	2,1%	7,7%	-5,2%	-17,2%
12	+0.29 mmCu + 2.5 mmAl	-4,5%	31,5%	-26,9%	-35,8%	-2,0%	3,8%	-5,6%	-25,5%
13	+0.58 mmCu	-2,6%	35,0%	-26,9%	-35,1%	1,2%	30,8%	-22,7%	-31,1%

Source: from the Author (2023)

Additional filtration has shown unequivocal results regarding dose reduction, which encourages its use as a way to protect the patient. However, the IQ is degraded in the presence of the additional filtration. As expected, the increased filtration resulted in a decrease in the number of photons in the main beam, reducing the signal level. However this reduction in signal value is at most 4.5% for ladder and 2% for plate, referring to FI12. This may indicate compensation by the SD and its signal pre-processing and image post-processing systems. Even in the presence of a thicker Cu filter (0.58 mmAl), referring to FI13 the variation in the average signal value for ROI#5 and ROI#12 was less than 3% and 2%, respectively.

Given also the smaller number of available photons there is always a greater statistical variation, and the noise values related to the degradation of the image increased as a function of the FI, but not uniformly with increasing filter thickness. This may be due both to small variations in the definition of each ROI in the image, and also, and mainly, to the pre- and post-processing mechanisms of the CR system that are automated. It can be seen that

the influence of the 0.29 mmCu and 0.58 mmCu filter on the increase in noise was 18% and 35%, respectively. However, for FI6 (2.5 mmAl) on the ladder almost the same noise value as the reference image was achieved (0.2%) and a small increase for ROI#12 (plate) and ROI#11 (background) of 2.2% and 2.5%, respectively compared to the reference image.
Figure 5 graphically depicts the ladder contrast curves as a function of FI versus the standard curve without filtration.

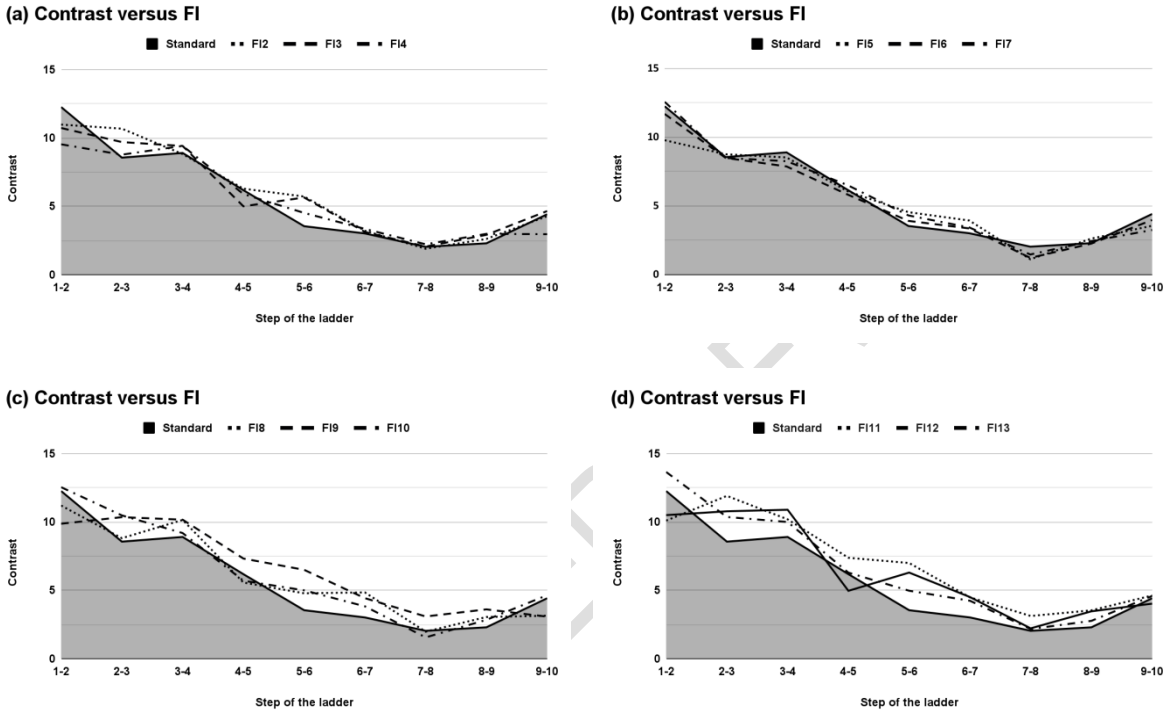

Fig. 5 - Ladder contrast curves as a function of FI.

Source: from the Author (2023). Figure (5a), compares the average contrast values (curve) of the reference image (Standard FI1) with the results of FI2, FI3 and FI4. Figure (5b), compares the standard FI1 curve with the results of FI5, FI6 and FI7. Figure (5c) compares the FI1 standard curve with the results of FI8, FI9 and FI10. Figure (5d), compares the FI1 standard curve with the results of FI11, FI12 and FI13.

The contrast difference referring to the adjacent steps of the ladder, after the addition of filters, a reduction was observed for the initial steps (lower thickness) and an increase for the final steps (higher thickness), which was expected due to beam hardening, from the analysis of the graphs in Figure (5a), (5b), (5c) and (5d).
Overall, for all contrast curves compared to the reference image, it was identified that the contrast increased with filtration, i.e. for a structure of the same density as the ladder, a small difference in thickness (2.9mm) between steps 5-6, the radiographic contrast increases for all FI.
On the other hand, for a structure of different densities (aluminum and water) a reduction in contrast between the plate and the hole is observed as a function of filtration, this drop was

5% for FI2 (+0.5 mmAl), a peak is noticed (contrast improvement) for FI6 that presented the smallest variation 3%, then reduced up to 30% for FI13 (+0.58 mmCu), staying at 14% and 21% for FI7 (+0.29 mmCu), FI8 (+0.29 mmCu + 0.5 mmAl), respectively.

3.3 Absorbed dose and effective dose

The mean mean absorbed dose (D) values for the main internal organs (bone marrow, ovaries, testicles, and bladder) in mGy and effective dose (E) in mSv for the radiographic examination of the pelvis according to ICRP 103 [16] and their respective deviations for each FI are shown in Table 6.

Table 6 - Mean dose (D) in internal organs (mGy) and effective dose (mSv) according to ICRP 103 [16] and respective percentage deviations as a function of FI

FI	bone marrow		ovaries		testicles		bladder		(ICRP 103)	
	mGy	D%	mGy	D%	mGy	D%	mGy	D%	mSv	D%
1	0,091	-	0,543	-	1,982	-	1,296	-	0,255	-
2	0,085	-6,6%	0,504	-7,2%	1,763	-11,0%	1,182	-8,8%	0,233	-8,6%
3	0,080	-12,1%	0,478	-12,0%	1,600	-19,3%	1,100	-15,1%	0,217	-14,9%
4	0,075	-17,6%	0,445	-18,0%	1,450	-26,8%	1,011	-22,0%	0,199	-22,0%
5	0,071	-22,0%	0,417	-23,2%	1,315	-33,7%	0,933	-28,0%	0,184	-27,8%
6	0,064	-29,7%	0,378	-30,4%	1,160	-41,5%	0,836	-35,5%	0,165	-35,3%
7	0,041	-54,9%	0,234	-56,9%	0,563	-71,6%	0,460	-64,5%	0,092	-63,9%
8	0,036	-60,4%	0,202	-62,8%	0,482	-75,7%	0,396	-69,4%	0,080	-68,6%
9	0,034	-62,6%	0,194	-64,3%	0,460	-76,8%	0,379	-70,8%	0,076	-70,2%
10	0,032	-64,8%	0,180	-66,9%	0,425	-78,6%	0,352	-72,8%	0,070	-72,5%
11	0,031	-65,9%	0,177	-67,4%	0,415	-79,1%	0,345	-73,4%	0,069	-72,9%
12	0,029	-68,1%	0,164	-69,8%	0,380	-80,8%	0,317	-75,5%	0,064	-74,9%
13	0,020	-78,0%	0,110	-79,7%	0,231	-88,3%	0,200	-84,6%	0,041	-83,9%

Source: from Author (2023). *The largest standard deviation was 2.2% for FI7 and the others were below 1%.

The results shown in Table 6 showed that for the same FI the average absorbed dose to the internal organs was lower for the testes, bladder, ovaries, bone marrow, respectively.

The results achieved in this study are in line with other studies, and encourages the use of additional filtration as a way to protect the patient. In 2011, Brosi et al. [17] were able to reduce the dose to the patient by 44% using a 0.3 mmCu plate and considered that Cu filters can help protect the superficial organs.

In 2005 a literature review article on dose optimization showed that for pelvis examinations with 66 kVp and 32 mA.s technique resulted in an effective dose (E) of 0.254 mSv which corroborates the value found in our study [18].

Compared to other authors, Palop et al. [19], and Hart, Hillier, and Shrimpton [20], currently in place the effective dose values 0.370 and 0.280 mSv, respectively. In this study we obtained 0.255 mSv without filtration and 0.064 mSv for FI13, corresponding to 0.58 mmCu which were lower than the corresponding values of the studies.

Other optimization studies consider radiation dose and IQ descriptors separately; however Barba; Culp [4], proposed a method to combine IQ and radiation dose data, the IQ descriptors are divided by the radiation dose to give a FOM. Figure 6 plots the FOM values for ladder and plate as a function of FI, a pattern of two regions with little variation in values

is observed, followed by two steps that stand out due to the cutoff in dose by the copper filter.

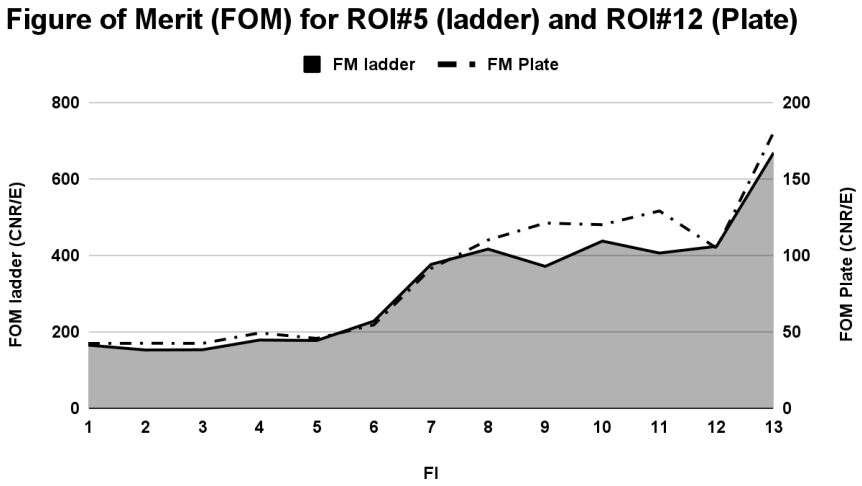

Fig. 6 - Figure of Merit Optimization for ladder (ROI#5) and plate (ROI#12).

Source: from the Author (2023).

Analyzing the FOM, represented in Figure 6, it was observed that for the additional filtrations of 0.58 mmCu, referring to FI13, was the best result, i.e., a reduction of greater than 92.1% in dose and 83.9% in effective dose, the reduction of the average absorbed dose in the internal organs, bone marrow, ovaries, testes and bladder were, 78.0%, 79.7%, 88.3% and 79.6%, respectively, however, there was a significant loss in IQ. The CRR worsened by an average of 35% compared to the reference image.

Indexes 9, 10, 11 and 12 showed a plateau with the best FOM values, the effective dose reductions were, 70.2%, 72.5%, 72.9% and 74.9% respectively. However, there was a worsening in the CNR 30% on average, compared to the OS reference image.

For indices 7 and 8 there was an expressive reduction in K_{AIR} and effective dose by 79.3% and 82.3%, 63.9% and 68.6%, respectively. For index 7 (0.29 mmCu), a reduction in mean absorbed dose in the internal organs of bone marrow, ovaries, testes and bladder were 54.9%, 56.9%, 71.6% and 64.5%, respectively, associated with a reduction in IQ of 17.8% and 23% in the ladder and plate CNR, respectively. For index 8 (0.29 mmCu + 0.5 mmAl), a reduction in K_{AIR}, mean absorbed dose in internal organs in the bone marrow, ovaries, testes and bladder were, 60.4%, 62.8%, 75.7% and 69.4%, versus the largest loss in QI of 21% and 16.4% in the CNR of the ladder and plate, respectively.

The smaller Indices present another plateau with the worst FOM values, Indices 2, 3, 4, 5, and 6. Among them FI6 (2.5 mmAl) which showed the best cost benefit ratio, i.e. dose versus IQ, which reduced K_{AIR} by 49.8% in the patient, 41.5% in the testes, 35.5% in the bladder, 30.4% in the ovaries, 29.7% in the bone marrow, and 35.3% in the patient's total effective dose for the pelvis scan, against the highest loss in IQ of 10.8% and 17.3% in the ladder and plate CNR, respectively.

Looking at IQ, the filtration option would be to use a few aluminum foils, for the FI6 (2.5 mmAl) with dose and IQ reduction of 50% versus 20%. On the other hand, from the standpoint of a steeper dose reduction, the option would be for FIs larger and equal to 7 (0.29 mmCu) with dose reduction greater than 80% versus 30%. According to Weis (2011) highlights that values below 10% represent negligible reductions and, those greater than 20%, present high losses in IQ.

4. CONCLUSION

It was verified by FOM that by keeping fixed the electric factors of the X-ray tube (70 kVp and mAs32) one can optimize the pelvis radiographic exam by the use of additional filtration, depending on the diagnostic IQ criteria established in the service. Thus, according to the results obtained it can be stated that the use of additional filtration of 2.5 mmAl was the best cost-benefit ratio, i.e. dose versus IQ for the pelvis examination, was reduced the K_{AIR} by 49.8% (1.64 to 0.82) mGy in the patient, 41.5% (1.982 to 1.160) mGy in the testes, 35.5% (1.296 to 0.836) mGy in the bladder, 30.4% (0.543 to 0.378) mGy in the ovaries, 29.7% (0.091 to 0.064) mGy in the bone marrow, and 35.3% (0.255 to 0.165) mSv the total effective dose of the examination with equivalent IQ.

REFERENCES

[1] Chan, C. T. P., & Fung, K. K. L. (2015). Dose optimization in pelvic radiography by air gap method on CR and DR systems–A phantom study. *Radiography*, *21*(3), 214-223.

[2] Alzyoud, K., Hogg, P., Snaith, B., Flintham, K., & England, A. (2019). Impact of body part thickness on AP pelvis radiographic image quality and effective dose. *Radiography*, *25*(1), e11-e17.

[3] Hamid, H. O. (2020). Evaluation of patient radiation dose in routine radiographic examinations in Saudi Arabia. *Radiation Physics and Chemistry*, *173*, 108883.

[4] Barba, J., & Culp, M. (2015). Copper filtration and kVp: effect on entrance skin exposure. *Radiologic technology*, *86*(6), 603-609.

[5] Jang, J. S., Yang, H. J., Koo, H. J., Kim, S. H., Park, C. R., Yoon, S. H., ... & Do, K. H. (2018). Image quality assessment with dose reduction using high kVp and additional filtration for abdominal digital radiography. *Physica Medica*, *50*, 46-51.

[6] Peacock, N. E., Steward, A. L., & Riley, P. J. (2020). An evaluation of the effect of tube potential on clinical image quality using direct digital detectors for pelvis and lumbar spine radiographs. *Journal of medical radiation sciences*, *67*(4), 260-268.

[7] WAYNE R. Software para processamento e análise de imagens. USA: National Institute of Mental Health, Java. 2021.

[8] Tavares, A., Lança, L., & Machado, N. (2015). Effect of technical parameters on dose and image quality in a computed radiography system.

[9] Tompe, A., & Sargar, K. (2021). X-Ray Image Quality Assurance. In *StatPearls [Internet]*. StatPearls Publishing.

[10] LOTUS HEALTHCARE. User's Manual HF 630M LOTUS healthcare. 2021. Available at: https://www.lotushealthcare.com.br/conjunto-hf-500m Accessed on: Nov. 20, 2021.

[11] AGFA. Computed Radiography Solutions. 2021. Available at: https://medimg.agfa.com/brazil/computed-radiography/ Accessed on: 20. Nov. 2021.

[12] RAYSAFE. Unfors RaySafe Xi. 2021. Available at: *https://www.raysafe.com/products/x-ray-test-equipment/raysafe-xi* Accessed on: 20. Nov. 2021.

[13] Tapiovaara, M., Lakkisto, M., & Servomaa, A. (1997). *PCXMC. A PC-based Monte Carlo program for calculating patient doses in medical x-ray examinations* (No. STUK-A--139). Finnish Centre for Radiation and Nuclear Safety (STUK).

[14] BRAZIL. Constitution (2019). Resolution - RDC No. 330, of December 20, 2019. 249. ed. Brasília, DF: Agência Nacional de Vigilância Sanitária, 26 Dec. 2019. Section 1, p. 92.

[15] WEIS, Guilherme Lopes et al. (2011). Reduction of radiation dose to patients and medical teams by the use of additional copper and aluminum filters in the outputs of X-ray

tubes in hemodynamic equipment. Dissertation (Master in Production Engineering) - Universidade Federal de Santa Maria, Rio Grande do Sul.
[16] Valentin, J. (2007). International Commission on Radiological Protection. The 2007 recommendations of the international commission on radiological protection. *Annals of the ICRP, ICRP Publication*, *103*, 2-4.
[17] Brosi, P., Stuessi, A., Verdun, F. R., Vock, P., & Wolf, R. (2011). Copper filtration in pediatric digital X-ray imaging: its impact on image quality and dose. *Radiological physics and technology*, *4*, 148-155.
[18] Tingberg, A., & Sjöström, D. (2005). Optimisation of image plate radiography with respect to tube voltage. *Radiation protection dosimetry*, *114*(1-3), 286-293.
[19] Vilar-Palop, J., Vilar, J., Hernández-Aguado, I., González-Álvarez, I., & Lumbreras, B. (2016). Updated effective doses in radiology. *Journal of radiological Protection*, *36*(4), 975.
[20] Hart, D., Hillier, M., & Shrimpton, P. (2010). Doses to Patients from Radiographic and Fluoroscopic X-ray Imaging Procedures in the UK. *Chilton: Health Protection Agency Centre for Radiation, Chemical and Environmental Hazards*.